Heterogeneous Catalysis

DOI: 10.1002/ange.201209255

Macro- and Mesoporous Polymers Synthesized by a CO_2-in-Ionic Liquid Emulsion-Templating Route**

Li Peng, Jianling Zhang, Jianshen Li, Buxing Han, Zhimin Xue, and Guanying Yang*

Porous polymers have received much interest because of their wide range of applications in catalysis, gas separation, structure replication, electrode materials, etc.[1] It is particularly appealing to synthesize macro- and mesoporous polymers because the hierarchical porous structures have the advantages of each class of the hierarchical pores and offer transport and diffusion pathways, especially for larger guest species.[2] Generally, macro- and mesoporous polymers are prepared using the direct synthesis methodology by reaction-induced phase separation.[3]

Emulsion templating is a useful method for the preparation of porous polymers.[4] Usually, oil-in-water or water-in-oil emulsions are used for emulsion polymerization.[5] Interestingly, Cooper et al. developed a CO_2-in-water emulsion-templating route for the synthesis of porous polymers.[6] The removal of the droplet phase is simple because CO_2 can revert to the gaseous state upon depressurization. Moreover, the CO_2-in-water emulsion[7] is more attractive than the conventional emulsions consisting of water and oil because CO_2 is nontoxic, inexpensive, and nonflammable.[8] The CO_2-in-water emulsion allows the production of hydrophilic polymers with porous structure.[6]

In recent years, ionic liquids (ILs) have received tremendous attention owing to their negligible vapor pressures, high chemical and thermal stability, wide liquid temperature range, and wide electrochemical windows.[9] Most importantly, ILs can solvate a wide range of organic and inorganic reagents.[10] ILs have been widely utilized as promising media in different fields, such as chemical reactions,[11] including polymerization.[12] However, their use for the synthesis of porous polymers is not widely reported.[13]

Herein, we propose for the first time a CO_2-in-IL emulsion templating route for the synthesis of porous polymers. The polymerization is initiated by UV irradiation to attain a fast polymerization rate.[14] Highly porous polyacrylamide (PAM) and poly(trimethylolpropane trimethacrylate) (PTRM) having hierarchical macro- and mesoporous structures were obtained, and the porosity properties can be easily tuned by the control of the CO_2 pressure. The as-synthesized polymers combine the advantages of both meso- and macropores, and have shown application potential in catalysis.

The emulsion formation in the CO_2/*N*-ethyl perfluorooctylsulfonamide (N-EtFOSA)/1-butyl-3-methylimidazolium nitrate ([bmim]NO_3) system was studied in the pressure range of 10–16 MPa at 25 °C (for structures of N-EtFOSA and IL [bmim]NO_3 see Figure S1 in the Supporting Information). The volume fraction of IL was fixed at 35 vol% and the surfactant concentration was 5.0 wt% based on the IL. A white, opaque emulsion was formed upon stirring, and filled the entire optical vessel (see Figure S2 in the Supporting Information). The emulsions were stable for about 2 hours after stirring was stopped. The electrical conductivity measurements show that the emulsions are highly conducting (see Figure S3 in the Supporting Information), thus representing IL-continuous (CO_2-in-IL) emulsions. Because the surfactant N-EtFOSA is much more soluble in the IL than in CO_2, the IL-continuous emulsion is favored. When acrylamide (monomer), benzophenone (initiator), and *N*,*N*′-methylenebisacrylamide (crosslinker) for the PAM synthesis were added to the emulsion, no remarkable change in the stability of the emulsion was observed.

The CO_2-in-IL emulsion containing acrylamide, benzophenone, and *N*,*N*′-methylenebisacrylamide was exposed to UV irradiation for 1 hour. Then CO_2 was released and the product was obtained after washing and drying. As an example, Figure 1 shows the SEM images of the PAM synthesized within the emulsion at 12.4 MPa. The macropores, which are about 3.5 μm in diameter, are distributed

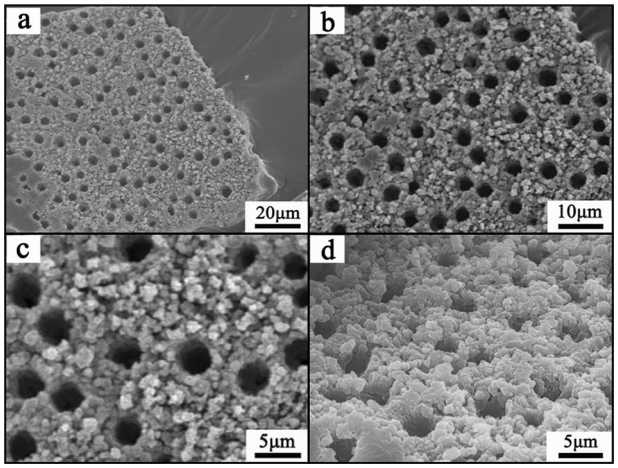

Figure 1. SEM images of the PAM synthesized in a CO_2-in-IL emulsion at 12.4 MPa and 25 °C.

[*] L. Peng, Prof. J. Zhang, J. Li, Prof. B. Han, Z. M. Xue, G. Yang
Beijing National Laboratory for Molecular Sciences, CAS Key Laboratory of Colloid and Interface and Thermodynamics, Institute of Chemistry, Chinese Academy of Sciences (China)
E-mail: zhangjl@iccas.ac.cn

[**] The authors thank the National Natural Science Foundation of China (21173238, 21133009, 21073207), Ministry of Science and Technology of China (2009CB930802), and the Chinese Academy of Sciences (KJCX2.YW.H16) for support.

Supporting information for this article is available on the WWW under http://dx.doi.org/10.1002/anie.201209255.

© 2013 Wiley-VCH Verlag GmbH & Co. KGaA, Weinheim

uniformly throughout the product. These macropores result from the templating effect of the CO_2 droplets during the polymerization, which occurs in the continuous IL phase. The polymer particles (100–300 nm) are packed loosely, thus generating smaller and irregular pores with sizes in the hundreds of nanometers range. The FT-IR spectra indicate the successful formation of the PAM and the thermogravimetric analysis shows that it is stable up to 260 °C (see Figures S4 and S5 in the Supporting Information).

The macroporosity of the PAM was determined by the mercury porosimetry method. The macropore size distribution curve of the PAM shows a pore size distribution centered at 3.4 μm (Figure 2 A), which is consistent with that observed

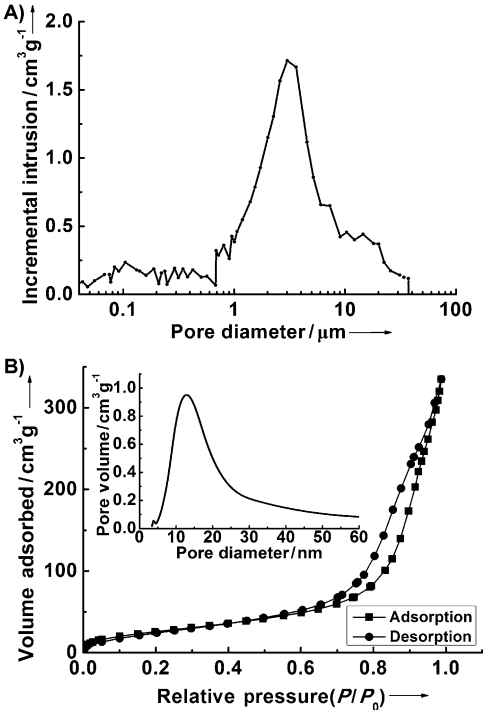

Figure 2. A) Macropore size distribution and B) the N_2 adsorption/desorption isotherm of the PAM synthesized at 12.4 MPa and 25 °C. The inset in B) shows the mesopore size distribution curve.

from the SEM images. The PAM has a total macropore volume of 4.03 $cm^3 g^{-1}$ and a porosity degree of 84.8 %. It is very interesting that the porosity degree of PAM is considerably higher than the volume fraction of CO_2 in the emulsion (65 vol % internal phase). For the polymer synthesized in the CO_2-in-water emulsion, the degree of porosity can be equal to the volume ratio of the internal phase when the original emulsion structure was completely retained during polymerization.[6b] Herein, the excess porosity higher than the volume fraction of CO_2 can be attributed to the templating effect of the IL during polymerization.[13] The release of the IL after polymerization generates excess macropores, which may correspond to the pores with sizes in the hundreds of nanometers range, as shown in the SEM images (Figure 1).

The mesoporosity of the PAM was determined by an N_2 adsorption/desorption method. As shown in Figure 2 B, the N_2 adsorption/desorption isotherm exhibits a mode of the type IV, which is related to mesoporous materials. The BET (Brunauer, Emmett, and Teller) surface area and total pore volume are 143.0 $m^2 g^{-1}$ and 0.473 $cm^3 g^{-1}$, respectively, and the mesopore size distribution curve, calculated from Barrett-Joyner-Halenda method, shows a pore size distribution centered at around 12.6 nm (inset of Figure 2 B). The mesopores in the PAM may result from the templating effect of the micelles formed from the surfactant in the IL.[15]

The PAMs were synthesized in CO_2-in-IL emulsions at different pressures, with all other experimental parameters being the same as those above. The products were characterized by FT-IR, mercury porosimetry, and N_2 adsorption/desorption methods. The results show that all the PAMs present hierarchical macro- and mesoporous structures (see Figures S6–S8 in the Supporting Information). Table 1 lists

Table 1: Effect of pressure on the porosity, total macropore volume (V_{pore}), median macropore diameter (D_{macro}), BET surface area (S_{BET}), mesopore volume (V_t), and mesopore diameter (D_{meso}) of the PAMs synthesized in CO_2-in-IL emulsion.

Pressure [MPa]	Porosity[a] [%]	V_{pore}[a] [$cm^{-3} g^{-1}$]	D_{macro}[a] [μm]	S_{BET}[b] [$m^2 g^{-1}$]	V_t[b] [$cm^{-3} g^{-1}$]	D_{meso}[b] [nm]
10.3	86.4	3.80	2.1	152.3	0.491	13.1
12.4	84.8	4.03	3.4	143.0	0.473	12.6
14.0	86.5	5.28	7.2	89.0	0.258	6.4
16.0	87.5	6.84	13.9	46.8	0.105	4.7

[a] Measured by mercury intrusion porosimetry. [b] Measured by N_2 adsorption/desorption isotherm analysis.

the properties of the macro- and mesopores of the PAMs synthesized at different pressures. All these PAMs have a high degree of porosity (> 80 %). Interestingly, the pressure has opposing effects on the properties of the macro- and mesopores, that is, the higher pressure favors the formation of a PAM with larger macropores and smaller mesopores. From 10.3 to 16.0 MPa, the macropore diameter is increased from 2.1 to 13.9 μm, while the mesopore diameter reduces from 13.1 to 4.7 nm. The total macropore volume of the PAM synthesized at 16.0 MPa can be as large as 6.84 $cm^3 g^{-1}$, whereas the mesopore volume and surface area fall to 0.105 $cm^3 g^{-1}$ and 46.8 $m^2 g^{-1}$, respectively. The mechanism for the effect of pressure on the porosities of PAMs is discussed below. The above results indicate that the macro- and mesopore properties of PAMs synthesized in CO_2-in-IL emulsions can be easily tuned by controlling the CO_2 pressure.

A mechanism for the formation of macro- and mesoporous polymers by a CO_2-in-IL emulsion-templating route is proposed (Figure 3). In the emulsion, the CO_2 droplets (micron sized) are dispersed in the IL continuous phase, and thus coexisting with the micelles which usually have sizes on the nanometer scale (Figure 3 a). Owing to the good solvency of the IL towards the reactants and the poor solvency of CO_2, the reactants are solubilized in the IL where the polymerization will proceed. During the polymerization

 © 2013 Wiley-VCH Verlag GmbH & Co. KGaA, Weinheim

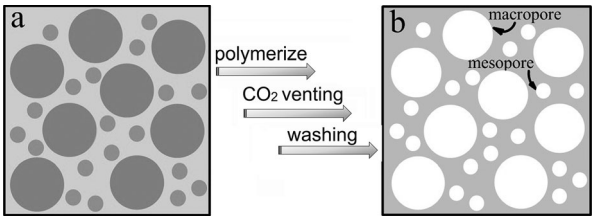

Figure 3. Schematic illustration for the formation of macro- and mesoporous polymers by using a CO_2-in-IL emulsion-templating route. The large and small spheres in a) represent the CO_2 droplets and micelles, respectively.

initiated by UV irradiation, the CO_2 droplets and micelles act as templates for the macro- and mesopore formation, respectively. Additionally, the IL plays a templating role during polymerization.[13] Therefore, the subsequent removal of CO_2, IL, and surfactant gives rise to the formation of a highly porous polymer with a hierarchical macro- and mesoporous structure (Figure 3b). At higher pressures, the surfactant becomes more CO_2 soluble, thus the interface is less curved about CO_2 and the CO_2 droplet size is increased.[7] Consequently, the PAMs synthesized at higher pressure has larger macropores because of the templating effect of the CO_2 droplets (Table 1). As for the reduced mesopore size of the PAMs made at higher CO_2 pressure (Table 1), it can be explained by the smaller micelle size at higher pressures, a phenomena which has been reported for CO_2-in-water micelles[16] and CO_2-in-IL micelles.[17]

The as-synthesized highly porous polymers have advantages of both mesopores and macropores, and thus have potential applications in catalysis. Herein we utilized the PAM as a support for a palladium catalyst. The Pd/PAM composite was synthesized and characterized by XRD, XPS, and EDX spectra (see Figures S9–S11 in the Supporting Information). The loading of palladium on the PAM was 3.1 wt% as determined by ICP-AES analysis. The catalytic performance of Pd/PAM for hydrogenation of styrene is shown in Table 2. Styrene was almost completely converted into ethylbenzene within 10 minutes at 30 °C and an H_2 pressure of 2 MPa when using a substrate/Pd molar ratio of 3200 (entry 1). The turnover frequency (TOF) was about 18000 h^{-1}. The Pd/PAM catalyst was reused twice for this reaction, and there was almost no activity loss (entries 2 and 3), thus indicating that the as-prepared catalyst is stable. For comparison, the styrene hydrogenation was performed using a commercial Pd/C catalyst under the same reaction conditions (Table 1, entries 4–6). The TOFs of the Pd/PAM are much higher than those of the commercial Pd/C catalyst. Additionally, we also performed the styrene hydrogenation using the Pd/PAM catalyst with an H_2 pressure of 1 atm at 25 °C (entries 7 and 8). The TOFs are also higher than those reported for Pd/polymer catalyst (entry 9).[18] These results indicate that the as-synthesized Pd/PAM catalyst has a much higher activity than the commercial Pd/C and the reported Pd/polymer for the hydrogenation of styrene.

Table 2: Catalytic activity test for the hydrogenation of styrene.[a]

Entry	p_{H_2}	t	Yield [%][b]	TOF[c]
1[d]	2 MPa	10 min	>99	18000
2[e]	2 MPa	10 min	>99	18000
3[e]	2 MPa	10 min	>99	18000
4[f]	2 MPa	10 min	85.93	10300
5[f]	2 MPa	15 min	93.45	7476
6[f]	2 MPa	20 min	>99	6000
7[d]	1 atm	6 h	88.02	1476
8[d]	1 atm	8 h	>99	1250
9[g]	1 atm	–	–	930

[a] Reaction conditions. Temperature: 30 °C for entries 1–6, 25 °C for entries 7–9. Substrate/Pd (mol/mol) = 3200 for entries 1–3. Substrate/Pd (mol/mol) = 2000 for entries 4–6). [b] Yield of ethybenzene. [c] Turnover number (TON) = mol of product (ethylbenzene) per mole of Pd; TOF = TON h^{-1}. [d] The Pd/PAM synthesized in this work. [e] The Pd/PAM was reused for 2 runs. [f] The commercial Pd/C catalyst. [g] The Pd/poly(phenyltriazolylmethyl)styrene reported in Ref. [18].

The Pd/PAM catalyst was also utilized for the Suzuki cross-coupling of iodobenzene with phenylboronic acid. The yield of biphenyl was enhanced about 14% in comparison to that obtained using the commercial Pd/C catalyst (see Table S1 in the Supporting Information). The high catalytic activity of the as-synthesized Pd/PAM catalyst may be ascribed to the hierarchical structure of the PAM. The macropores facilitate the mass transport and the mesopores increase the surface area for contact of the reactants with the palladium nanoparticles. Thus the Pd/PAM has high activity for the catalytic reaction.

Furthermore, the CO_2-in-IL emulsion-templating method was applied for the synthesis of a hydrophobic polymer, that is, the macro- and mesoporous PTRM was obtained (see SEM images and N_2 adsorption/desorption isotherm in Figures S12 and S13 in the Supporting Information). The data indicate that the CO_2-in-IL emulsion-templating route is versatile in synthesizing both hydrophilic and hydrophobic polymers, and can be attributed to the good solvency of the IL towards a wide range of reagents.

In summary, macro- and mesoporous polymers with high porosity have been synthesized by a CO_2-in-IL emulsion-templating route under UV radiation. The porosities of the polymers are easily tuned by controlling the CO_2 pressure. These porous materials combine the advantages of both meso- and macropores, and have potential applications in catalysis, gas separation, and material fabrication. The CO_2-in-IL emulsion-templating method can be applied to the synthesis of some other highly porous polymers.

Experimental Section

Emulsion formation and characterization: The apparatus consisted of a view cell (9.5 mL) equipped with two quartz view windows, a high-pressure pump, and a pressure gauge. In a typical experiment, 4.00 g of 5.0 wt% N-EtFOSA/[bmim]NO_3 solution was loaded into the view cell at 25 °C. The view cell was then charged with CO_2 to the desired pressure with stirring. The emulsion formation was observed at different pressures. The apparatus and procedure for conductivity measurement are given in the Supporting Information.

PAM synthesis and characterization: The monomer acrylamide (0.8 g), crosslinker *N*,*N*′-methylenebisacrylamide (0.04 g) and initiator benzophenone (0.04 g) were added into 5.0 wt% N-EtFOSA/[bmim]NO_3 solution (4.00 g), which was loaded in the view cell

© 2013 Wiley-VCH Verlag GmbH & Co. KGaA, Weinheim

(9.5 mL) equipped with quartz view windows at 25 °C. CO_2 was charged into the cell with stirring until the desired pressure was reached. The cell was radiated by two high-pressure mercury vapor lamps at wavelength of $\lambda = 254$ nm for 1 hour. Then CO_2 was released by depressurization. The white product was washed with ethanol and dried at 80 °C under vacuum for 24 h.

The morphologies of PAM were characterized by a HITACHI S-4800 SEM. The macroporosities were recorded by mercury intrusion porosimetry using a Micromeritics Autopore IV 9500 porosimeter. The samples were subjected to a pressure cycle starting at 5 psia, increasing to 44500 psia in predefined steps to give pore size/pore volume information. The mesoporosities were determined by N_2 adsorptio/desorption isotherms using a Quadrasorb SI-MP system. FT-IR spectra were obtained by a Bruker Tensor 27 spectrometer. The TG measurement was carried out using TA Q50 with N_2 flow of 40 mL min^{-1}.

Pd/PAM synthesis and catalytic activity: The PAM synthesized at 12.4 MPa (0.15 g) and $Pd(OAc)_2$ (0.016 g) was added into a flask containing 100 mL acetone. The flask was placed in an oil bath at 70 °C and the mixture was stirred for 24 h. After centrifugation, the product was dried and reduced at 150 °C for 2 h with H_2. Pd/PAM was obtained after cooling.

For the hydrogenation reaction, styrene (1 g), *n*-heptane (1 g), and Pd/PAM (10 mg) were placed in a 20 mL stainless steel reactor. The reactor was evacuated and filled with H_2 (three times). The stirrer was started with a rate of 300 rpm. H_2 was added to suitable pressure and kept to be constant during the reaction, which was monitored by a pressure transducer (Foxboro/ICT model 930). After reaction for a certain time, the product was separated with the catalyst by centrifugation (1200 rpm) and the product was analyzed by a gas chromatograph (Agilent 6820) equipped with a flame ionization detector (FID) and a PEG-20M capillary column (0.25 mm in diameter, 30 m in length). The experimental details for the Suzuki cross-coupling reaction catalyzed by Pd/PAM are shown in the Supporting Information.

Received: November 19, 2012
Published online: January 4, 2013

Keywords: heterogeneous catalysis · ionic liquids · mesoporous materials · palladium · polymers

[1] a) S. Kitagawa, R. Kitaura, S. Noro, *Angew. Chem.* **2004**, *116*, 2388; *Angew. Chem. Int. Ed.* **2004**, *43*, 2334; b) S. Kitagawa, K. Uemura, *Chem. Soc. Rev.* **2005**, *34*, 109; c) Y. Zhang, S. N. Riduan, *Chem. Soc. Rev.* **2012**, *41*, 2083; d) M. T. Gokmen, F. E. Du Prez, *Prog. Polym. Sci.* **2012**, *37*, 365.

[2] a) A. P. Côté, A. I. Benin, N. W. Ockwig, M. O'Keeffe, A. J. Matzger, O. M. Yaghi, *Science* **2005**, *310*, 1166; b) F. S. Macintyre, D. C. Sherrington, L. Tetley, *Macromolecules* **2006**, *39*, 5381; c) C. Zou, D. C. Wu, M. Z. Li, Q. C. Zeng, F. Xu, Z. Y. Huang, R. W. Fu, *J. Mater. Chem.* **2010**, *20*, 731; d) B. Li, R. Gong, Y. Luo, B. Tan, *Soft Matter* **2011**, *7*, 10910.

[3] D. Wu, F. Xu, B. Sun, R. Fu, H. He, K. Matyjaszewski, *Chem. Rev.* **2012**, *112*, 3959.

[4] a) H. F. Zhang, A. I. Cooper, *Soft Matter* **2005**, *1*, 107; b) N. R. Cameron, *Polymer* **2005**, *46*, 1439; c) P. B. Zetterlund, Y. Kagawa, M. Okubo, *Chem. Rev.* **2008**, *108*, 3747.

[5] a) Y. X. Liu, P. G. Jessop, M. Cunningham, C. A. Eckert, C. L. Liotta, *Science* **2006**, *313*, 958; b) A. Walther, M. Hoffmann, A. H. E. Mueller, *Angew. Chem.* **2008**, *120*, 723; *Angew. Chem. Int. Ed.* **2008**, *47*, 711; c) F. Schüler, D. Schamel, A. Salonen, W. Drenckhan, M. D. Gilchrist, C. Stubenrauch, *Angew. Chem.* **2012**, *124*, 2256; *Angew. Chem. Int. Ed.* **2012**, *51*, 2213.

[6] a) R. Butler, C. M. Davies, A. I. Cooper, *Adv. Mater.* **2001**, *13*, 1459; b) H. F. Zhang, G. C. Hardy, M. J. Rosseinsky, A. I. Cooper, *Adv. Mater.* **2003**, *15*, 78; c) R. Butler, I. Hopkinson, A. I. Cooper, *J. Am. Chem. Soc.* **2003**, *125*, 14473; d) B. Tan, J. Y. Lee, A. I. Cooper, *Macromolecules* **2007**, *40*, 1945; e) J. Y. Lee, B. Tan, A. I. Cooper, *Macromolecules* **2007**, *40*, 1955.

[7] a) S. R. P. da Rocha, J. Dickson, D. Cho, P. J. Rossky, K. P. Johnston, *Langmuir* **2003**, *19*, 3114; b) V. V. Dhanuka, J. L. Dickson, W. Ryoo, K. P. Johnston, *J. Colloid Interface Sci.* **2006**, *298*, 406; c) S. S. Adkins, D. Gohil, J. L. Dickson, S. E. Webber, K. P. Johnston, *Phys. Chem. Chem. Phys.* **2008**, *9*, 6333; d) E. Torino, E. Reverchon, K. P. Johnston, *J. Colloid Interface Sci.* **2010**, *348*, 469; e) S. S. Adkins, X. Chen, I. Chan, E. Torino, Q. P. Nguyen, A. W. Sanders, K. P. Johnston, *Langmuir* **2010**, *26*, 5335.

[8] a) C. A. Eckert, B. L. Knutson, P. G. Debenedetti, *Nature* **1996**, *383*, 313; b) E. J. Beckman, *Science* **1996**, *271*, 613; c) G. B. Jacobson, C. T. Lee, K. P. Johnston, W. Tumas, *J. Am. Chem. Soc.* **1999**, *121*, 11902; d) P. Raveendran, Y. Ikushima, S. L. Wallen, *Acc. Chem. Res.* **2005**, *38*, 478; e) P. G. Jessop, B. Subramaniam, *Chem. Rev.* **2007**, *107*, 2666; f) Q. L. Chen, E. J. Beckman, *Green Chem.* **2008**, *10*, 934.

[9] a) M. Smiglak, A. Metlen, R. D. Rogers, *Acc. Chem. Res.* **2007**, *40*, 1182; b) D. Chaturvedi, *Curr. Org. Chem.* **2011**, *15*, 1236; c) C. D. Hubbard, P. Illner, R. van Eldik, *Chem. Soc. Rev.* **2011**, *40*, 272; d) M. Petkovic, K. R. Seddon, L. P. N. Rebelo, C. S. Pereira, S. Cristina, *Chem. Soc. Rev.* **2011**, *40*, 1383.

[10] a) T. Welton, *Chem. Rev.* **1999**, *99*, 2071; b) W. Miao, T. H. Chan, *Acc. Chem. Res.* **2006**, *39*, 897.

[11] a) Q. H. Zhang, S. G. Zhang, Y. Q. Deng, *Green Chem.* **2011**, *13*, 2619; b) J. P. Hallett, T. Welton, *Chem. Rev.* **2011**, *111*, 3508.

[12] a) J. Lua, F. Yan, J. Texter, *Prog. Polym. Sci.* **2009**, *34*, 431; b) M. Patel, M. Gnanavel, A. J. Bhattacharyya, *J. Mater. Chem.* **2011**, *21*, 17419.

[13] a) P. Snedden, A. I. Cooper, K. Scott, N. Winterton, *Macromolecules* **2003**, *36*, 4549; b) L. Zhu, C. Y. Huang, Y. H. Patel, J. Wu, S. V. Malhotra, *Macromol. Rapid Commun.* **2006**, *27*, 1306; c) Y. H. Shih, B. Singco, W. L. Liu, C. H. Hsu, H. Y. Huang, *Green Chem.* **2011**, *13*, 296.

[14] a) S. Yamago, Y. Ukai, A. Matsumoto, Y. Nakamura, *J. Am. Chem. Soc.* **2009**, *131*, 2100; b) Y. H. Zhao, X. Y. Zhu, K. Wee, R. B. Bai, *J. Phys. Chem. B* **2010**, *114*, 2422; c) H. Han, J. Bissell, F. Yaghmaie, C. E. Davis, *Langmuir* **2010**, *26*, 515.

[15] a) L. G. Qiu, T. Xu, Z. Q. Li, W. Wang, Y. Wu, X. Jiang, X. Y. Tian, L. D. Zhang, *Angew. Chem.* **2008**, *120*, 9629; *Angew. Chem. Int. Ed.* **2008**, *47*, 9487; b) L. B. Sun, J. R. Li, J. Park, H. C. Zhou, *J. Am. Chem. Soc.* **2012**, *134*, 126; c) M. H. Pham, G. T. Vuong, F. G. Fontaine, T. O. Do, *Cryst. Growth Des.* **2012**, *12*, 1008.

[16] C. T. Lee, W. Ryoo, P. G. Smith, J. Arellano, D. R. Mitchell, R. J. Lagow, S. E. Webber, K. P. Johnston, *J. Am. Chem. Soc.* **2003**, *125*, 3181.

[17] J. L. Zhang, B. X. Han, J. S. Li, Y. J. Zhao, G. Y. Yang, *Angew. Chem.* **2011**, *123*, 10085; *Angew. Chem. Int. Ed.* **2011**, *50*, 9911.

[18] C. Ornelas, A. K. Diallo, J. Ruiz, D. Astruc, *Adv. Synth. Catal.* **2009**, *351*, 2147.

 © 2013 Wiley-VCH Verlag GmbH & Co. KGaA, Weinheim